Synthesis, Spectroscopic Properties, Anti-Breast Cancer and Anti-Microbial Studies of Some Metal Complexes for New Schiff Base Ligand Derived From Anthranilic Acid.

Hanan F. Abd El-Halim (hanan_farouk1@hotmail.com)
Misr International University
Gehad Mohamed
Cairo University
Walaa Mahmoud
Cairo University
Omnia El-Sayed
Cairo University

Research Article

Keywords: Schiff base complexes, anthranilic acid, dibenzoyl methane, antimicrobial activity, anticancer activity.

Posted Date: March 24th, 2021

DOI: https://doi.org/10.21203/rs.3.rs-341811/v1

Abstract

2,2′-((1Z-1′Z) (1,3-diphenylpropane-1,3-diylidene) bis (azanylylidene)) dibenzoic acid (H_2L) Schiff base ligand, was obtained by condensation reaction between anthranilic acid and dibenzoyl methane in 2:1 ratio.

A series of Cr(III), Mn(II), Fe(III), Co(II), Ni(II), Cu(II), Zn(II) and Cd(II) complexes was resulted from 1:1 (ligand: metal salt) reaction.

The structural features of the synthesized ligand and its metal complexes was determined by elemental analyses, IR, ^{1}H NMR, UV-Vis, ESR, mass spectra, conductivity and magnetic susceptibility measurements as well as thermal (TG/DTG) analyses.

The analytical and spectroscopic tools showed that the complexes had composition of ML type with octahedral geometry. The IR results confirmed the tetradendate binding of the ligand involving two azomethine nitrogen atoms and two carboxylate oxygens. The Schiff base and its complexes have been screened for their antimicrobial activity against several bacterial organisms as (*Streptococcus pneumoniae* and *Bacillus subtilis*; *Pseudomonas aeruginosa* and *Escherichia coli*) and fungi (*Aspergillus fumigatus*; *Syncephalastrum racemosum*; *Geotricum candidum* and *Candida albicans*) by disk diffusion method.

All the metal complexes have potent antimicrobial activity than the free ligand. Anticancer activity of the ligand and its metal complexes was evaluated against human cancer (MCF-7 cells viability).

Introduction

The Schiff base ligands are derived by the condensation of aldehyde/ketone with a primary amine, which play a pivotal role in human welfare and these are the essential ligands in modern coordination and medicinal chemistry. These compounds had been used for industrial purposes such as pigments, catalysts, intermediates in organic synthesis and as polymer stabilizers [1]. Various transition and inner-transition metal with bi, tri and tetradentate Schiff bases containing nitrogen and oxygen or sulfur donor atoms played an important role in biological systems [2-4].

The azomethine (-C=N-) linkage present in Schiff base ligand and its metal (II) complexes, has special importance in elucidating the mechanism of transmination and racemization in biological system. It showed a wide range of biocidal activities such as antibacterial, antifungal, herbicidal, anti-inflammatory, anticancer, anti-diabetic, antileishmanial and antitumor activities [5].

The aim of this work is to prepare a novel Schiff base ligand by condensation of *anthranilic acid* with dibenzoyl methane and its Cr(III), Mn(II), Fe(III), Co(II), Ni(II), Cu(II), Zn(II) and Cd(II) complexes. Characterization using different physico-chemical techniques was employed. The biological and anticancer activities of this Schiff base and its metal complexes were reported. Remarkable increase in the antimicrobial or anticancer activity was found upon introducing the metal ions to the ligand center. Suggested molecular structures of the metal complexes were performed.

Experimental

Materials and reagents:

All chemicals used were of the analytical reagent grade (AR), and of highest purity available. They included *anthranilic acid*, dibenzoyl methane, $CrCl_3.6H_2O$, $MnCl_2.2H_2O$, $FeCl_3.6H_2O$, $CoCl_2.6H_2O$, $NiCl_2.6H_2O$, $CuCl_2.2H_2O$, $ZnCl_2$ and $CdCl_2$ and they provided from Acros, Sigma, Prolabo, Aldrich, BDH, Merck, and Strem Chemicals.

Organic solvents used were ethyl alcohol (90%), acetone and dimethylformamide (DMF). Distilled water was usually used in all preparations.

Solutions

Stock solutions of the Schiff base ligand and its metal complexes of $1x10^{-3}$ M were prepared by dissolving an accurately weighed amount of the complex in dimethylformamide for measuring their UV-Vis spectra.

Solution of anticancer study

A fresh stock solution of $1x10^{-3}$ M of Schiff base ligand (0.0012 g/L) was prepared in the appropriate volume of ethanol (95%). Dimethylsulphoxide (DMSO) (Sigma Chemical Co., St. Louis, Mo, USA) was used in cryopreservation of cells. RPMI-1640 medium (Sigma Chemical Co., St. Louis, Mo, USA) was used. The medium was used for culturing and maintenance of the human tumor cell line. The medium was supplied in a powder form.

It was prepared by weighing 10.4 g medium which mixed with 2 g sodium bicarbonate, completed to 1 L with distilled water and shaked carefully till complete dissolution. The medium was then sterilized by filtration in a Millipore bacterial filter (0.22 lm). The prepared medium was kept in a refrigerator (4 ^oC) and checked at regular intervals for contamination. Before use, the medium was warmed at 37 ^oC in a water bath and supplemented with penicillin/streptomycin and Fetal Bovine Serum (FBS). Sodium bicarbonate (Sigma Chemical Co., St. Louis, Mo, USA) was used for the preparation of RPMI-1640 medium. 0.05% Isotonic Trypan blue solution (Sigma Chemical Co., St. Louis, Mo, USA) was prepared in normal saline and was used for viability counting. 10% FBS (heat inactivated at 56 ^oC for 30 min), 100 units/ml Penicillin and 2 mg/ml Streptomycin were supplied from Sigma Chemical Co., St. Louis, Mo, USA and were used for the supplementation of RPMI-1640 medium prior to use. 0.025% (w/v) Trypsin (Sigma Chemical Co., St. Louis, Mo, USA) was used for the harvesting of cells. 1% (v/v) Acetic acid (Sigma Chemical Co., St. Louis, Mo, USA) was used for dissolving the unbound SRB dye. 0.4% Sulphorhodamine-B (SRB) (Sigma Chemical Co., St. Louis, Mo, USA) dissolved in 1% acetic acid was used as a protein dye. A stock solution of trichloroacetic acid (TCA, 50%, Sigma Chemical Co., St. Louis, Mo, USA) was prepared and stored. 50 µl of the stock was added to 200 µl RPMI-1640 medium/well to yield a final concentration of 10% used for protein precipitation. 100% Isopropanol and 70% ethanol were used. Tris base 10 mM (pH 10.5) was used for SRB dye solubilization. 121.1 g of tris base was dissolved in 1000 ml of distilled water and pH was adjusted by HCl acid (2 M).

Instruments

Mass spectra were recorded by the EI technique at 70 eV using MS-5988 GS-MS Hewlett–Packard instrument at the Microanalytical Center, National Center for Research, Egypt.

The molar magnetic susceptibility was measured on powdered samples using the Faraday method. The diamagnetic corrections were made by Pascal's constant and $Hg[Co(SCN)_4]$ was used as a calibrant. Molar conductivities of 10^{-3} M solutions of the solid complexes in ethanol were measured using Jenway 4010 conductivity meter. The X-ray powder diffraction analyses were carried out using Philips Analytical X-ray BV,

diffractometer type PW 1840. Radiation was provided by copper target (Cu anode2000 W) high intensity X-ray tube operated at 40 KV and 25 mA. Divergence and the receiving slits were 1 and 0.2, respectively. Microanalyses of carbon, hydrogen and nitrogen were carried out at the Microanalytical Center, Cairo University, Egypt, using CHNS-932 (LECO) Vario Elemental Analyzer. Analyses of the metals followed the dissolution of the solid complexes in concentrated HNO_3, neutralizing the diluted aqueous solutions with ammonia and titrating the metal solutions with EDTA. FT-IR spectra were recorded on a Perkin-Elmer 1650 spectrometer (4000–400 cm^{-1}) in KBr pellets. Electronic spectra were recorded at room temperature on a Shimadzu 3101pc spectrophotometer as solutions in ethanol. ^1H NMR spectra, as a solution in DMSO-d_6, were recorded on a 300 MHz Varian-Oxford Mercury at room temperature using TMS as an internal standard. Electron spin resonance spectra were also recorded on JES-FE2XG ESR spectrophotometer at Microanalytical Center, Tanta University. UV-Vis spectra were carried out on UV mini-1240, UV-Vis spectrophotometer, Shimadzu. The thermogravimetric analyses (TG and DTG) of the solid complexes were carried out from room temperature to 1000 ^oC using a Shimadzu TG-50H thermal analyzer. The antimicrobial activities were carried out at the Microanalytical Center, Cairo University, Egypt. The anticancer activity was performed at the National Cancer Institute, Cancer Biology Department, Pharmacology Department, Cairo University. The optical density (O.D.) of each well was measured spectrophotometrically at 564 nm with an ELIZA microplate reader (Meter tech. R 960, USA).

Synthesis of Schiff base ligand

The Schiff base ligand (H_2L) was prepared by refluxing a mixture of dibenzoyl methane (17.83 mmol, 4 g) dissolved in acetone was added dropwise to *anthranilic acid* (35.65 mmol, 4.89 g) dissolved in ethanol. The resulting mixture was stirred under reflux for about 2 hours during which a greenish yellow solid compound was separated. It was filtered, recrystallized, washed with acetone and dried in vacuum.

The yellow Schiff base product was produced in 90.0% yield. M.p.: 64 °C; FT-IR (KBr, v cm^{-1}): (O-H) = 3372, (C=N) = 1612, (C=O) = 1671; ^{1} H NMR (300 MHz, DMSO, δ ppm): 12.98 (s, H, OH), 7.34 - 7.54 (m, 10H, Ar H benzoyl methane), 7.57 - 8.18 (m, 8H, Ar H amino benzoic acid), 4.87(s, 2H, CH_2). The molecular ion peak was found at m/z = 461.78 amu. Anal. calcd for H_2L: C, 75.30; H, 4.50; N, 6.04, Found: C, 75.32; H, 4.70; N, 6.06.

Synthesis of metal complexes

The Cr(III), Mn(II), Fe(III), Co(II), Ni(II), Cu(II), Zn(II) and Cd(II) complexes were prepared by reaction of 1:1 molar mixture of hot ethanolic solution (60 ^oC) of the metal chloride ($8.65x10^{-4}$ mol) and the ligand (H_2L) (0.4 g, $8.65x10^{-4}$ mol). The resulting mixture was stirred under reflux for 1 hour whereupon the complexes precipitated. They were collected by filtration, purified by washing several times with hot ethanol.

$[Cr(L)(H_2O)_2]Cl$, Yield: (87%); Green colour; m.p: 100 °C; μeff (B.M) 4.10; Λm ($Ω^{-1}$ mol^{-1} cm^2) 70.0; FT-IR (KBr, v cm^{-1}): (OH) = 3382, (C=O) = 1694, (C=N) = 1605, $(COO)_{asym}$ = 1533, $(COO)_{sym}$ = 1407, (M-O) = 564, (M-N) = 431. Anal. Calcd: C, 59.64; H, 4.11; N, 4.79; Cr, 8.91; Found: C, 59.36; H, 4.03; N, 4.56; Cr, 8.78.

$[Mn(L)(H_2O)_2]$, Yield: (85%); Brown colour; m.p: 110 °C; μeff (B.M) 5.98; Λm ($Ω^{-1}$ mol^{-1} cm^2) 8.0; FT-IR (KBr, v cm^{-1}): (OH) = 3472, (C=O) = 1668, (C=N) = 1591, $(COO)_{asym}$ = 1543, $(COO)_{sym}$ = 1458, (M-O) = 556, (M-N) = 452. Anal. Calcd: C, 63.16; H, 4.35; N, 5.089; Mn, 9.90; Found: C, 63.09; H, 4.06; N, 5.05, Mn, 9.95.

[Fe(L)$(H_2O)_2$]Cl, Yield: (80%); Brown colour; m.p: 118 °C; μeff (B.M) 5.08;Λm ($Ω^{-1}$ mol^{-1} cm^2) 67.0; FT-IR (KBr, v cm^{-1}): (OH) = 3426, (C=O) = 1697, (C=N) = 1591, $(COO)_{asym}$ = 1526, $(COO)_{sym}$ = 1480, (M-O) = 564, (M-N) = 488. Anal. Calcd: C, 55.21; H, 3.32; N, 4.43; Fe, 9.51; Found: C, 55.11; H, 3.14; N, 4.16, Fe, 9.08.

[Co(L)$(H_2O)_2$], Yield: (82%); Brown colour; m.p: 170 °C; μeff (B.M) 4.97;Λm ($Ω^{-1}$ mol^{-1} cm^2) 35.0; FT-IR (KBr, v cm^{-1}): (OH) = 3402, (C=O) = 1689, (C=N) = 1592, $(COO)_{asym}$ = 1537, $(COO)_{sym}$ = 1408, (M-O) = 562, (M-N) = 419. Anal. Calcd: C, 62.71; H, 4.32; N, 5.04; Co, 10.61; Found: C, 62.41; H, 4.17; N, 5.01, Co, 10.76.

[Ni(L)$(H_2O)_2$], Yield: (87%); Green colour; m.p: ›300 °C; μeff (B.M) 3.44;Λm ($Ω^{-1}$ mol^{-1} cm^2) 30.0; FT-IR (KBr, v cm^{-1}): (OH) = 3403, (C=O) = 1691, (C=N) = 1594, $(COO)_{asym}$ = 1540, $(COO)_{sym}$ = 1406, (M-O) = 564, (M-N) = 494. Anal. Calcd: C, 62.73; H, 4.30; N, 5.04; Ni, 10.85; Found: C, 62.45; H, 4.23; N, 5.00, Ni, 10.55.

[Cu(L)$(H_2O)_2$]H_2O, Yield: (80%); Black green colour; m.p: 110 °C; μeff (B.M) 1.68; Λm ($Ω^{-1}$ mol^{-1} cm^2) 38.0; FT-IR (KBr, v cm^{-1}): (OH) = 3403, (C=O) = 1690, (C=N) = 1594, $(COO)_{asym}$ = 1525, $(COO)_{sym}$ = 1455, (M-O) = 586, (M-N) = 422. Anal. Calcd: C, 60.25; H, 4.50; N, 4.84; Cu, 11.00; Found: C, 60.16; H, 4.36; N, 4.59, Cu, 10.98.

[Zn(L)$(H_2O)_2$], Yield: (86%); Brown colour; m.p: 148 °C; μeff (B.M) diamagnetic; Λm ($Ω^{-1}$ mol^{-1} cm^2) 11.0; FT-IR (KBr, v cm^{-1}): (OH) = 3499, (C=O) = 1606, (C=N) = 1560, $(COO)_{asym}$ = 1508, $(COO)_{sym}$ = 1488, (M-O) = 583, (M-N) = 468. Anal. Calcd: C, 61.98; H, 4.27; N, 4.98; Zn, 11.64; Found: C, 61.63; H, 4.01; N, 4.53, Zn, 11.34.

[Cd(L)$(H_2O)_2$], Yield: (83%); Brown colour; m.p: 220 °C; μeff (B.M) diamagnetic; Λm ($Ω^{-1}$ mol^{-1} cm^2) 11.0; FT-IR (KBr, v cm^{-1}): (OH) = 3473, (C=O) = 1671, (C=N) = 1589, $(COO)_{asym}$ = 1555, $(COO)_{sym}$ = 1418, (M-O) = 566, (M-N) = 416. Anal. Calcd: C, 57.19; H, 3.94; N, 4.60; Cd, 18.47; Found: C, 57.02; H, 3.90; N, 4.35, Cd, 18.08.

Biological activity

Antimicrobial activity

A filter paper disk (5 mm) was transferred into 250 ml flasks containing 20 ml of working volume of tested solution (100 mg/ml). All flasks were autoclaved for 20 min at 121°C. LB agar media surfaces were inoculated with four investigated bacteria (Gram positive bacteria: *Streptococcus pneumoniae* and *Bacillus Subtilis*; Gram negative bacteria: *Pseudomonas aeruginoa* and *Escherichia coli* and fungi *Aspergillus fumigatus*; *Syncephalastrum racemosum*; *Geotricum candidum* and *Candida albicans*) by diffusion agar technique [6-8] then, transferred to a saturated disk with a tested solution in the center of Petri dish (agar plates). All the compounds were placed at 4 equidistant places at a distance of 2 cm from the center in the inoculated Petri plates. DMSO served as control. Finally, all these Petri dishes were incubated at 25 °C for 48 h where clear or inhibition zones were detected around each disk. Control flask of the experiment was designed to perform under the same condition described previously for each microorganism but with DMSO solution only and by subtracting the diameter of inhibition zone resulting with DMSO from that obtained in each case, so antibacterial activity could be calculated [9,10]. Amikacin and ketoconazole were used as reference compounds for antibacterial and antifungal activities, respectively. All experiments were performed as triplicate and data plotted were the mean value.

Anticancer activity

Potential cytotoxicity of the compounds was tested using the method of Skehan and Storeng [9]. Cells were plated in 96-multiwell plate (104 cells/well) for 24 h before treatment with the compounds to allow attachment of cell to the wall of the plate. Different concentrations of the compounds under investigation (0, 5, 12.5, 25, 50 and 100 µg/ml) were added to the cell monolayer triplicate wells were prepared for each individual dose. The monolayer cells were incubated with the compounds for 48 h at 37 ^{o}C and in 5% CO_2 atmosphere. After 48 h, cells were fixed, washed and stained with SRB stain. Excess stain was washed with acetic acid and attached stain was recovered with tris–EDTA buffer. The optical density (O.D.) of each well was measured spectrophotometrically at 564 nm with an ELIZA microplate reader and the mean background absorbance was automatically subtracted and mean values of each drug concentration was calculated. The relation between surviving fraction and drug concentration is plotted to get the survival curve of Breast tumor cell line for each compound.

Calculation:

The percentage of cell survival was calculated as follows:

Survival fraction = O.D. (treated cells)/O.D. (control cells).

The IC_{50} values (the concentrations of symmetric Schiff base ligand or its complexes required to produce 50% inhibition of cell growth) were calculated. The experiment was repeated three times for MCF7 cell line.

Results And Discussion

3.1- Characterization of the Schiff base ligand.

The Schiff base ligand prepared by the reaction of *anthranilic acid* with dibenzoyl methane in a molar ratio 2:1. The ligand was yellowish stable powder at room temperature. It was soluble in common organic solvents.

The results of elemental analysis obtained were in good agreement with those calculated for the suggested formula indicating that the ligand had the molecular formula $C_{29}H_{22}N_2O_4$, table 1.

The IR spectrum of H_2L ligand showed the presence of new strong and sharp vibration band at 1612 cm^{-1} referring to the azomethine group v(C=N), corresponding to the formation of the Schiff base [11].

^{1}H NMR spectrum was used to ensure ligand structure and purity in *d6*-dimethylsulfoxide (DMSO-d_6) solution using Me_4Si (TMS) as internal standard [12]. The multiple in the region 7.34-8.18 ppm may be assigned to aromatic ring protons while the carboxylic acid group was given as sharp singlet at 12.98 ppm.

The mass spectrum of the H_2L ligand was characterized by the molecular ion peak appeared at (m/z) 461.78 amu confirming the proposed formula in which the ligand moiety was $C_{29}H_{22}N_2O_4$ with atomic mass 462 amu.

The structure of the symmetric Schiff base ligand under study was shown in Figure 1.

3.2-Characterization of metal complexes

All the complexes were colored and stable to air and moisture. They were soluble in DMF. The complexes were characterized by different techniques such as elemental analyses, IR spectra, mass, ^{1}H NMR and thermal analyses.

3.2.1-Elemental analyses of complexes

Metal complexes were synthesized by the reaction of the Schiff base dissolved in hot acetone with an ethanolic solution of the corresponding metal salt in a molar ratio 1:1. The experimental elemental analysis of complexes was in good compliance with the theoretical calculations. The elemental analyses of metal complexes (C, H, N and M) with molecular formula and the melting point were illustrated in Table 1.

3.2.2. Spectral studies

3.2.2.1. IR spectral studies

The IR spectra of the complexes were compared with those of the free ligand to determine the involvement of coordination sites in chelation, listed in Table 2. The IR spectra of the ligand H_2L exhibited a band at 1612 cm^{-1} due to the azomethine v(C=N) group [13,14], which was shifted to lower frequencies in the spectra of all the complexes (1548 – 1605) cm^{-1} [15]. These bands were shifted to lower wave numbers indicating the involvement of azomethine nitrogen in coordination to the metal ions [16]. A carbonyl v(C=O) vibration band which appeared in the IR spectrum of the ligand H_2L at 1671 cm^{-1} similarly underwent a shift into lower or higher frequency (1606 – 1697) cm^{-1} in the complexes [17]. Strong bands corresponding to $v_{asym}(COO^-)$ and $v_{sym}(COO^-)$ vibrations of the free ligand was observed at 1558 cm^{-1} and 1419 cm^{-1}, respectively [18]. On complexion in this study, the asymmetric carboxylate stretching $v_{asym}(COO^-)$ was shifted to the (1480 - 1555) cm^{-1} and the symmetric carboxylate stretching $v_{sym}(COO^-)$ was shifted (1400 - 1488) cm^{-1} ; indicating the linkage between the metal ions and carboxylate oxygen atom [19]. The spectra of the complexes showed broad bands in the 3382-3499 cm^{-1} range attributed to the stretching vibration of the v (OH) of the carboxylic group in the spectra of the metal complexes while appeared at 3372 cm^{-1} in the spectrum of the Schiff base ligand [20]. The presence of bands in all complexes in the region 416-494 cm^{-1} originated from v(M-N) azomethine vibrational mode [21]. The bands present in the region 556-583 cm^{-1} in all the complexes were assignable to v(M-O) stretching vibration [12]. In addition, two bands of coordinated water molecules $\nu(H_2O)$ appeared in the IR spectra of metal complexes at 917-950 and 834-871 cm^{-1}, indicating the binding of water molecules to the metal ions [22]. The new weak intensity bands of (M-O) stretching vibrations occur at 516-545 cm^{-1}. Accordingly, the ligand acted as tetradendate chelating agent, bonded to the metal ion via two carboxylate oxygen and two azomethine nitrogen atoms of the Schiff base. The formation of octahedral complexes was brought through coordination by two water molecules in all complexes.

3.2.2.2. ^{1}H NMR spectral studies of H_2L and its complexes

The ^{1}H NMR spectra of the Schiff base ligand and its Zn(II) and Cd(II) complexes were recorded in DMSO-d_6 by using tetramethylsilane (TMS) as internal standard. The chemical shifts of the different types of protons in the ^{1}H NMR spectra of the Schiff base and its complexes were listed in Table 3. The protons of an aromatic ring showed in the range of 7.34 -7.54 ppm [23], while appeared at 6.46 - 7.51 and 6.26 - 7.53 ppm in $[Zn(L)(H_2O)_2]$ and $[Cd(L)(H_2O)_2]$ complexes, respectively. The disappearance of the COOH signal in the spectra of the $[Zn(L)(H_2O)_2]$ and $[Cd(L)(H_2O)_2]$ complexes relative to free Schiff base at 12.98 ppm indicated that the ligand acted as di-negative ligand which undergoes deprotonation during complexation process [24].

3.2.2.3-Mass analysis

The mass spectra of the Cu(II) and Fe(III) complexes revealed the molecular ion peaks at m/z 576.77 and 586.58 amu, respectively, which were consistent with the calculated weight 577.55 and 587.34 amu, respectively. These data confirmed the stoichiometry of these complexes as being of [ML] type.

3.2.2.4. Electronic spectral studies and magnetic susceptibility

Electronic spectra of H_2L and its complexes were recorded at room temperature. The spectrum of H_2L showed band at 263 nm, assigned to π → π* transitions of the aromatic rings. In addition, strong bands also appeared at 342 nm assignable to n → π* transition of the azomethine group. Due to the coordination of azomethine nitrogen to the metal centers showed bands which shifted to 253 - 346 nm for π → π* transition and 341 - 537 nm for n → π* transition [25].

The diffused reflectance spectrum of Cr(III) complex exhibited three bands at 28,530 25,252 and 19,157 cm^{-1} which may be assigned to the $^4A_{2g}(F) \rightarrow {}^4T_{2g}(F)$, $^4A_{2g}(F) \rightarrow {}^4T_{1g}(F)$ and $^4A_{2g}(F) \rightarrow {}^4T_{2g}(P)$ spin allowed d-d transitions, respectively. The magnetic moment value was found to be 4.10 B.M. which indicated the presence of Cr(III) complex in octahedral geometry [26].

Manganese(II) complex exhibited four intensity absorption bands in the ranges 16,366; 22,371; 25,445; 37,174 cm^{-1}, which may be assigned to the transitions: $^6A_{1g} \rightarrow {}^4T_{1g}$ (4G), $^4A_{1g}$(4G) (10B + 5C), $^6A_{1g} \rightarrow {}^4E_g$, $^6A_{1g} \rightarrow {}^4E_g$ (4D) (17B + 5C), $^6A_{1g} \rightarrow {}^4T_{1g}$ (4P) (7B + 7C) , respectively [27]. The magnetic moment value was found to be 5.98 B.M; which indicated the presence of Mn(II) complex in octahedral structure [28].

From the diffuse reflectance spectrum, it was observed that the Fe(III) chelate exhibited a band at 37,453 cm^{-1}, which may be assigned to the $^6A_{1g} \rightarrow T_{2g}$(G) transition in the octahedral geometry of the complex [29]. The $^6A_{1g} \rightarrow {}^5T_{1g}$ transition appeared to be split into two bands at 26,666 cm^{-1} and 22,883 cm^{-1}. The spectrum also showed a band at 47,846 cm^{-1}, which may be attributed to ligand to metal charge transfer. The observed magnetic moment of Fe(III) complex was 5.08 B.M which confirmed the octahedral geometry.

The diffused reflectance spectrum of cobalt(II) complex showed three bands in the 16,366, 17,376, and 21,008 cm^{-1} regions assignable to the $^4T_{1g})F(\rightarrow {}^4T_{2g})F(;\ ^4T_{1g})F(\rightarrow {}^4A_{2g})F(;$ and $^4T_{1g})F(\rightarrow {}^4T_{1g})P($ transitions, respectively, corresponding to the octahedral geometry around the Co(II) ion [28]. The observed magnetic moment value of 4.97 B.M. correspond to high spin state and further support the octahedral geometry around Co(II) ion.

The diffused reflectance spectral data of Ni(II) complex showed d-d bands in the region 16,694,18.115 and 25,740 cm^{-1}, respectively [30], assigned to $^3A_{2g}(F) \rightarrow {}^3T_{2g}(F)$, $^3A_{2g}(F) \rightarrow {}^3T_{1g}(F)$ and $^3A_{2g}(F) \rightarrow {}^3T_{2g}(F)$ transitions, which were characteristic of Ni(II) in octahedral geometry [31]. The Ni(II) complex exhibited magnetic moment value of 2.44 BM attributed to two unpaired electrons per Ni(II) ion suggesting that this complex has an octahedral geometry [32].

Diffused reflectance spectrum of Cu(II) complex showed the d-d transition bands in the range of 16,406, 19,569 and 26,809 cm^{-1} [33]. These bands correspond to $^2B_{1g} \rightarrow {}^2A_{1g}$ ($d_{x2-y2} \rightarrow d_{z2}$), $^2B_{1g} \rightarrow {}^2B_{2g}$ ($d_{x2-y2} \rightarrow d_{xy}$) and $^2B_{1g} \rightarrow {}^2E_g$ ($d_{x2-y2} \rightarrow d_{xz}$, d_{yz}) transitions, respectively. On the basis of electronic transitions, a distorted octahedral geometry was suggested for Cu(II) complex [31]. The obtained magnetic moment value of 2.68 BM for Cu(II) complex was indicative of one unpaired electron per Cu(II) ion for d^9-system suggesting spin-free distorted octahedral geometry

[31]. Both of Zn(II) and Cd(II) complexes were diamagnetic, which according to the empirical formulae, an octahedral geometry was proposed for these chelates.

3.2.2.5. Electron spin resonance spectrum of Cu(II) complex

The ESR spectra of metal complexes provided information about hyperfine and superhyperfine structures, which are of importance in studying the metal ion environment in the complex, i.e., the geometry, nature of ligating sites of Schiff base and metal, and the degree of covalency of metal–ligand bonds [16]. The ESR spectrum for copper(II) complex at room temperature consisted of two signals, one with four hyperfine-structure lines at low magnetic field (the $g_{\parallel}$ signal) and the other at high field ($g_{\perp}$ signal) [33]. The trend $g_{\parallel} > g_{\perp}$ > free electron-spin (2.0023), indicated that the unpaired electron was localized in d_{x2-y2} orbital of the Cu(II) ion [34] and the spectral figure was characteristic for distorted octahedral sites (D_{4h}) [35]. The spectrum of $[Cu(L)(H_2O)_2]H_2O$ complex was given in Figure 2 which exhibited a broad $g_{\perp}$ component, with splitting of $g_{\parallel}$ component, reflecting the coupling with the Cu(II) nucleus (I= 3/2), the $g_{\parallel}$ value at 2.12 and $g_{\perp}$ at 1.96 [36]. It had reported that $g_{\parallel}$ was less than 2.3 for covalent character and greater than 2.3 for ionic character of the metal ligand bond in the complexes [16]. According to Hathaway [37, 38], the parameter G, determined as $G = (g_{\parallel} - 2) / (g_{\perp} - 2)$, if G was greater than 4, the exchange interaction may be negligible; however, if G is less than 4, a considerable exchange interaction was indicated in the solid complex [39, 40]. The calculated G value for the Cu(II) complex was 3.2, indicative of considerable exchange interaction between the copper centers in the solid [40].

3.2.3. Molar conductance measurements

The measured molar conductance values of 10^{-3} M metal complexes in DMF at 25 ^{o}C were listed in Table 1. The Cr(III) and Fe(III) complexes had molar conductance values of 70 and 67 Ω^{-1} mol^{-1} cm^2, respectively, indicating the ionic nature of these complexes and they were electrolytes. The rest of prepared complexes were non-electrolytes (Table 1).

3.2.4. Thermal analysis studies (TG and DTG)

The thermal studies of ligand and its metal complexes were carried out using the thermogravimetric technique (TG) and differential thermogravimetric (DTG) analyses. The thermal analysis gives useful data for the thermal stability of the metal complexes. The TG and DTG was recorded within the temperature range from 30 to 1000 °C (Table 4).

The Schiff base ligand (H_2L) with the molecular formula ($C_{29}H_{22}N_2O_4$) was thermally decomposed in two successive decomposition steps. The first and second steps with estimated mass loss of 99.92% (calculated mass loss = 98.71%) within the temperature range 152 - 367 ^{o}C may be attributed to the loss of $C_{29}H_{22}N_2O_4$ molecule. The DTG curve gave two maximum peaks temperature at 182 - 352 ^{o}C. The overall weight loss amounts to 99.92% (calculated mass loss = 98.71%).

Thermogravimetric (TG) curve for $[Cr(L)(H_2O)_2]Cl$ complex showed three weight loss events. The first and second steps of decomposition occurred within the range of 134 – 250 ^{o}C, with two maxima at 150 and 222 ^{o}C and corresponded to the loss of two molecules of coordinated water, HCl molecule, CO_2 gas and C_7H_3N fragment with an estimated mass loss of 36.54% (calculated mass loss = 37.27%). The final step occurred within the range of 385 - 470 ^{o}C which corresponded to loss of $C_{18}H_{16}NO_{0.5}$ fragment with estimated mass loss 43.38% (calculated mass

loss = 43.53%) leaving behind ½Cr_2O_3 contaminated with carbons as the product of decomposition. The overall weight loss amounts to 79.93% (calculated mass loss = 80.80%).

The TG curve of [Mn(L)$(H_2O)_2$] complex was thermally decomposed in two successive decomposition steps. The first and second stages of decomposition occurred in the range of 152-499 °C with two maximum temperatures at 189 and 453 ^oC represented the loss of two H_2O molecules, carbon dioxide gas and $C_{25}H_{20}N_2O$ fragment with an estimated weight loss of 80.19% (calculated mass loss = 80.58%). MnO contaminated with carbon was the residue of decomposition.

Thermogravimetric (TG) curve for [Fe(L)$(H_2O)_2$]Cl chelate showed three weight loss events. The first step of decomposition occurred in the range of 121 - 232 ^oC with maximum temperature at 169 ^oC and corresponded to the loss of two molecules of coordinate water, carbon dioxide gas, HCl molecule and C_6H_3N fragment with estimated mass loss 35.25% (calculated mass loss = 34.98%). The second and third steps occurred within the range of 366 – 586 °C with two maxima temperatures at 401 and 557 ^oC which corresponded to loss of $C_{19}H_{16}NO_{0.5}$ fragment with estimated mass loss 45.18% (calculated mass loss = 45.28%) leaving metal oxide ½Fe_2O_3 contaminated with carbons as residue. The overall weight loss amounts were 80.43% (calculated mass loss = 80.26%).

[Co(L)$(H_2O)_2$] complex gave decomposition pattern of two stages. The first stage within the temperature range of 144 – 208 °C with maximum temperature 173 °C was related to the evolution of two H_2O molecules, CO_2 gas and $C_{13}H_9N$ fragment with an estimated mass loss of 46.86 % (calcd. = 46.67 %). The final decomposition stage occurred in the temperature range from 360 to 432 ^oC with one maximum at 392 ^oC. The estimated mass loss of 31.55% (calculated mass loss = 31.53%) was reasonably for complete decomposition of CO gas and a part of ligand $C_{10}H_{13}N$ and leaving CoO contaminated with carbons as final product. The overall weight loss amounted to 78.41 % (calcd. 78.20 %).

The [Ni(L)$(H_2O)_2$] complex decomposed from temperature 144 to 425 ^oC with two steps as follows. The first step occurred within the temperature range of 144 - 265 ^oC with maximum temperature at 172 ^oC and correspond to elimination of two water molecules, carbon dioxide gas and a part of ligand molecule ($C_{14}H_{11}N$) with a found mass loss of 49.32 % (calcd. = 49.21 %). The second step represented the loss of CO gas and $C_{10}H_9N$ molecule with a mass loss of 31.40% (calcd. = 30.82%) and the temperature range 366 - 425 ^oC with maxima at 400 ^oC. At the end of the thermogram, the metal oxide NiO contaminated with carbons was the residue with total estimated mass loss of 80.72% (calcd. = 80.03%).

[Cu(L)$(H_2O)_2$]H_2O complex was thermally decomposed in three steps within the temperature range from 66 to 346 ^oC. The first decomposition step with an estimated mass loss of 3.22 % (calcd. = 3.11%) occurred within the temperature range from 66 to 115 ^oC with maximum temperature at 89 ^oC. The second and third decomposition steps occurred within the range of 135 – 346 °C with two maximum temperatures at 168 and 304 ^oC. These steps may be attributed to elimination of two molecules of coordination water and CO_2 gas and $C_{24}H_{20}N_2O$ fragment leaving CuO contaminated with carbons as residues. The overall weight loss amounts to 77.83 % (calcd. 77.90 %).

The [Zn(L)$(H_2O)_2$] chelate gave decomposition pattern of three stages. The first stage occurred within the temperature range of 172-211°C with maximum temperature at 190 ^oC. This step related to the evolution of two molecules of coordinate water, CO_2 gas and a part of ligand ($C_{13}H_9N$) molecule with a found mass loss of 45.71%

(calcd. = 46.13%). The last two decomposition stages within the temperature range of 341-651 °C with two maxima temperature at 352 and 623 ^{o}C, in which the complex losses carbon monoxide gas and $C_{10}H_{11}N$ fragment with estimated mass loss 30.38% (calcd. = 30.81%). At the end of the thermogram, the metal oxide ZnO and four carbons as final product with total estimated mass loss of 76.10% (calcd. = 76.94%).

$[Cd(L)(H_2O)_2]$ complex was thermally decomposed in one step within the temperature range from 155 to 239 ^{o}C with maximum temperature at 195 ^{o}C. This step involved complete evaluation of two molecules of coordinate water, carbon dioxide gas and ligand $C_{27}H_{20}N_2O$ molecule with estimated mass loss of 76.52% (calcd. = 76.92%) and leaving CdO contaminated with carbon as residue.

3.2.5-Structural interpretation

The structures of the Schiff base ligand (H_2L) with Cr(III), Mn(II), Fe(III), Co(II), Ni(II), Cu(II), Zn(II) and Cd(II) complexes were characterized by elemental analyses, molar conductance, magnetic, solid reflectance and thermal analysis data. From IR spectra, it could be concluded that H_2L behaved as a di-negatively tetradentate ligand coordinated to the metal ions via two nitrogen atoms of azomethine group and two oxygen atoms of carboxylate group. From the molar conductance data, it was found that the complexes are non-electrolytes expect Cr(III) and Fe(III) complexes. The structure was given in Figure (3).

3.3.1. Biological activity

The higher activity of metal complex was probably due to greater lipophilic nature of the complex. It can be explained on the basis of Overtone's concept and Tweedy's chelation theory [41]. According to Overtone's concept of cell permeability, the lipid membrane that surrounds the cell favors the passage of only lipid soluble materials due to which liposolubility was considered to be an important factor that controls the antimicrobial activity. On chelation, the polarity of the metal ion will be reduced to a greater extent due to the overlap of the ligand orbital and partial sharing of positive charge of metal ion with donor groups. Further, it increased the delocalization of the π electrons over the whole chelate ring and enhanced the lipophilicity of the complex. This increased lipophilicity enhanced the penetration of the complexes into lipid membrane and thus blocked the metal binding sites on enzymes of microorganisms. These metal complexes also disturb the respiration process of the cell and thus block the synthesis of proteins, which restrict further growth of the organism. There were other factors which also increased the activity as: solubility, conductivity and bond length between the metal and ligand [42 - 44].

Antifungal and antibacterial activity in vitro using four fungi species (*Aspergillus fumigatus; Syncephalastrum racemosum; Geotricum candidum* and *Candida albicans*) and two bacteria – Gram-negative (*Pseudomonas aeruginosa* and *Escherichia coli*) and Gram-positive bacteria (*Streptococcus pneumoniae* and *Bacillus Subtilis*) were assessed for the Schiff base as well as its metal complexes [45].

Measurement of zone of inhibition against the growth of bacteria and fungi for the ligand (H_2L) and its metal complexes was shown in Figures (4,5) and Table (5). DMSO was used as a negative control and amikacin and ketoconozole drugs were used as positive standards for antibacterial and antifungal studies [22].

The antibacterial studies showed that, using *Streptococcus pneumoniae* as *Gram-positive bacteria*, the biological activity of the Ni(II), Cu(II), Cd(II), Fe(III) and Cr(III) complexes were higher than that of the free H_2L ligand. While the Mn(II) complex had the same biological activity of free H_2L ligand. The biological activity of the Co(II) and Zn(II)

complexes were lower than that of the free H_2L ligand. Using *Bacillus Subtilis* as *Gram-positive bacteria*, the biological activity of Cu(II), Ni(II), Fe(III), Cr(III), Cd(II) and Co(II) complexes were higher than that of the free H_2L ligand. While the biological activity of the Mn(II) and Zn(II) complexes were lower than free H_2L ligand. The study on *Pseudomonas aeruginosa* as *Gram-negative bacteria,* revealed that the biological activity of Ni(II), Fe(III), Cu(II), Co(II), Cr(III) were higher than that of the free H_2L ligand. While the Cd(II), Zn(II), Mn(II) had the same biological activity as that of free H_2L ligand. Using *Escherichia coli* as *Gram-negative bacteria,* the biological activity of Fe(III), Ni(II), Cu(II), Cd(II), Co(II) and Cr(III) were higher than that of the free H_2L ligand. For Zn(II) complex, its biological activity was the same like the free H_2L ligand. While the Mn(II) complex had lower biological activity than that the free H_2L ligand.

The antifungal studies showed, by using *Candida albicans fungus*, that the biological activity of the Cr(III), Ni(II), Cu(II), Mn(II), Zn(II) and Fe(III) complexes were higher than that the free H_2L ligand. While the biological activity of Cd(II) and Co(II) complexes were lower than that of the free H_2L ligand. Using *Geotricum candidum fungus*, the biological activity of all metal complexes was higher than that free H_2L ligand. While the highest biological activity was found for Cu(II) complex and the lowest activity was Co(II) and Fe(III) complexes. Using *Syncephalastrum racemosumfungus,* there isn't biological activity of the free H_2L ligand but the Zn(II) complex had the highest activity and the Ni(II) complex had the lowest activity. Using *Aspergillus fumigatus fungus,* the highest biological activity was found for the Zn(II) complex and the lowest activity was the Cu(II) complex. However, no significant activity has been observed for the free H_2L ligand.

The activities of the prepared Schiff base ligand and its metal complexes were confirmed by calculating the activity index according to the following relation [46, 47]:

$$\text{Activity index (A)} = \frac{\text{Inhibition Zone of compound (mm)}}{\text{Inhibition Zone of standard drug (mm)}} \times 100$$

From the data, it was concluded that Cu(II) complex had the highest activity index, while Fe(III) complex had the lowest activity index as shown in Figure (6).

3.3.2. Anticancer activity evaluation

The ligand and its complexes were investigated for their anticancer activity against human breast cancer cell line MCF 7. The range of inhibition of cell growth of ligand and its complexes between 33-56%. The results of inhibition of cell growth lower than 70% so we didn't make further testing with different concentration.

Conclusion

Preparation and characterization of the new Cr(III), Mn(II), Fe(III), Co(II), Ni(II), Cu(II), Zn(II) and Cd(II) complexes with the Schiff base ligand H_2L 2,2'-((1Z-1'Z)-(1,3-diphenyl propane-1,3diylidene) bis (azanylylidene)) dibenzoic acid was studied. The ligand acted as binegative tetradentate through two azomethine nitrogens and two carboxylate oxygens and all complexes showed octahedral geometry. All complexes were non-conductive expect Fe(III) and Cr(III) complexes were conductive, with the type of 1:1 electrolyte. From the data of elemental analysis, the complexes had composition of the ML type with general formulae $[M(L)(H_2O)_2]$ (M = Mn(II), Cu(II), Ni(II), Co(II), Zn(II) and Cd(II)) and $[M(L)(H_2O)_2]Cl_n$ (M = Cr(III) and Fe(III), n = 1). The biological activities of some complexes

were higher than free Ligand. The Cu(II) complex had the highest activity index, while Fe(III) complex had the lowest activity index. The free ligand and its complexes didn't show any anticancer activity.

References

1. **P.** Przybylski, A. Huczynski, K. Pyta, B. Brzezinski, F. Bartl, Biological properties of Schiff bases and azo derivatives of phenol. Curr. Org. Chem,**13,** 124-148(2009).
2. S. Malik, S. Ghosh, L. Mitu, Complexes of some 3d-metals with a Schiff base derived from 5-acetamido-1,3,4-thiadiazole-2-sulphonamide and their biological activity. J. Serb. Chem. Soc. ,**76**, 1387–1394(2011).
3. N. Raman, S. Raja, J. Joseph, J. Raja, Synthsis, spectral characterization and DNA cleavage study of heterocyclic Schiff base metal complexes. J. Chil. Chem. Soc, **52**, 1138-1141(2007).
4. M. Alias, H. Kassum, C. Shakir, Synthesis, physical characterization and biological evaluation of Schiff base M(II) complexes. Journal of the Association of Arab Universities for Basic and Applied Science,15, 28-34(2014).
5. P. Subbaraj, A. Ramu, N. Raman, J. Dharmaraja, Synthesis, characterization, DNA interaction and pharmacological studies of substituted benzophenone derived Schiff base metal(II) complexes. *J. Saudi Chem. Soc.,* 19, 207-216(2015).
6. M. Pfaller, L. Burmeister, M. Bartlett, M. Rinaldi, Multicenter evaluation of four methods of yeast inoculum preparation. *J. Clin. Microbiol*, **26**, 1437- 1441(1988).
7. National Committee for Clinical Laboratory Standards. Reference method for broth dilution antifungal susceptibilty testing of conidium-forming filamentous: proposed standard M38-A. Wayne, PA, USA (2002).
8. National Committee for Clinical Laboratory Standards. Method for antifungal disc diffusion susceptibility testing of yeast: proposed guideline M44-P, Wayne, PA, USA (2003).
9. P. Skehan, R. Storeng, et al., New colorimetric cytotoxicity assay for anticancer-drug screening. J. Natl. Cancer Ins.**, 82**, 1107-1112(1990).
10. I. Sakıyan, E. Loğoğlu, et al., Antimicrobial activities of N-(2-hydroxy-1-naphthalidene) -amino acid (glycine, alanine, phenylalanine, histidine, tryptophane) Schiff bases and their manganese(III) complexes. *BioMetals*, **17**, 115-120(2004).
11. M. Azam, S.M. Wabaidur, et al., Synthesis, characterization, cytotoxicity, and molecular docking studies of ampyrone-based transition metal complexes, Transition Metal Chemistry, 46,65–71(2021).
12. G. Kumar, S. Devi, D. Kumar, Synthesis of Schiff base 24-membered trivalent transition metal derivatives with their anti-inflammation and antimicrobial evaluation. J. Molecular Structure**, 1108**, 680- 688(2016).
13. Z. Guo, R. Xing, et al., The synthesis and antioxidant activity of the Schiff bases of chitosan and carboxymethyl chitosan. Bioorganic & Medicinal Chemistry Letters, 15, 4600-4603(2005).
14. Neelima, K. Poonia, et al., In vitro anticancer activities of Schiff base and its lanthanum complex. J. Spectrochimica Acta Part A, 155, 146-154(2016).
15. P. Ajibade, G. Kolawole, et al., Cobalt(II) complexes of the antibiotic sulfadiazine, the X-ray single crystal structure of $[Co(C_{10}H_9N_4O_2S)_2(CH_3OH)_2]$. Inorganica Chimica Acta*, **359**,* 3111-3116(2006).
16. N. Mahalakshm, R. Rajavel, Synthesis, spectroscopic, DNA cleavage and antibacterial activity of binuclear Schiff base complexes. Arabian Journal of Chemistry, 7, 509- 517(2014).
17. L. Li, B. Fu, et al., Synthesis, characterization and cytotoxicity studies of platinum(II) complexes with reduced amino acid ester Schiff-bases as ligands J. Inorganica Chimica Acta, **419**,135-140(2014).

18. R. Gnanasambandam, A. Proctor, Determination of pectin degree of esterification by diffuse reflectance Fourier transform infrared spectroscopy. J. Food Chemistry,68, 327-332(2000).
19. M.S. Nair, R.S. Joseyphus, Synthesis and characterization of Co(II), Ni(II), Cu(II) and Zn(II) complexes of tridentate Schiff base derived from vanillin and DL-alpha-aminobutyric acid. J. Spectrochimica Acta Part A,**70,** 749-753(2008).
20. T.T. Liu, Y.W. Tseng, T.S. Yang, Functionalities of conjugated compounds of γ-aminobutyric acid with salicylaldehyde or cinnamaldehyde. J. Food Chemistry, 190,1102-1108(2016).
21. A.Z. El-Sonbati, M.A. Diab, A.A. El-Bindary, et al. Geometrical structures, thermal stability and antimicrobial activity of Schiff base supramolecular and its metal complexes. J. Molecular Liquids, **215**, 423-442(2016).
22. C.M. Sharaby, Synthesis, spectroscopic, thermal and antimicrobial studies of some novel metal complexes of Schiff base derived from [N1-(4-methoxy-1,2,5-thiadiazol-3-yl) sulfanilamide] and 2-thiophene carboxaldehyde. J. Spectrochim. Acta A, 66,1271-1278(2007).
23. M. Mahmoud, S. Zaitone, et al. Synthesis, structure and antidiabetic activity of chromium(III) complexes of metformin Schiff-bases. J. Molecular Structure, 1108, 60-70(2016).
24. E.M. Zayed, E.H. Ismail, G.G. Mohamed, et al. Synthesis, spectroscopic and structural characterization, and antimicrobial studies of metal complexes of a new hexadentate Schiff base ligand. Spectrophotometric determination of Fe(III) in water samples using a recovery test, J. Monatsh Chem,145,755-765(2014).
25. S. Shit, A. Sasmal, P. Dhal, et al. Syntheses, structural variations and fluorescence studies of two dinuclear zinc(II) complexes of a Schiff base ligand with an extended carboxylate side arm, J. Molecular Structure,1108, 475-481(2016).
26. W.H. Mahmoud, G.G. Mohamed, M.M.I. El-Dessouky, Synthesis, structural characterization, in vitro antimicrobial and anticancer activity studies of ternary metal complexes containing glycine amino acid and the anti-inflammatory drug lornoxicam, J. Molecular Structure,1082,12-22(2015).
27. R. Kumar, S. Chandra, Spectroscopic techniques and cyclic voltammetry with synthesis: Manganese(II) coordination stability and its ligand field parameters effect on macrocyclic ligands, J. Spectrochimica Acta Part A, **67**, 188-195(2007).
28. N.A. Mangalam, S.R. Sheeja, M.R.P. Kurup, Mn(II) complexes of some acylhydrazones with NNO donor sites: Syntheses, a spectroscopic view on their coordination possibilities and crystal structures, J. Polyhedron, 29, 3318-3323(2010).
29. F.A. Cotton, G. Wilkinson, C.A. Murillo, M. Bochmann, Advanced Inorganic Chemistry, 6^{th} ed., Wiley, New York (1999).
30. H.F. Abd El-Halim, G.G. Mohamed, Synthesis, spectroscopic, thermal analyses, biological activity and molecular docking studies on mixed ligand complexes derived from Schiff base ligands and 2,6-pyridine dicarboxylic acid, Appl Organometal Chem, 32, 4176-4192(2018).
31. P. Tyagi, S. Chandra, B.S. Saraswat, D. Sharma, Design, spectral characterization, DFT and biological studies of transition metal complexes of Schiff base derived from 2-aminobenzamide, pyrrole and furan aldehyde, J. Spectrochimica Acta Part A,**143**, 1-11(2015).
32. S. Chandraa, Ruchi, K. Qanungo, S.K. Sharma, Synthesis, molecular modeling and spectroscopic characterization of nickel(II), copper(II), complexes of new 16-membered mixed-donor macrocyclic schiff base ligand incorporating a pendant alcohol function, J. Spectrochimica Acta Part A, **79**, 1326-1330(2011).
33. D. Kivelson, R. Neiman, ESR Studies on the Bonding in Copper Complexes, J. Chem. Phys., 35, 149(1961).

34. A. A. El-Bindary, A.Z. El-Sonbati, et al. Polymeric complexes — LXII. Coordination chemistry of supramolecular Schiff base polymer complexes - A review, J. Molecular Liquids**, 216**, 318-329(2016).
35. N. Raman, S.J. Raja, DNA cleavage, structural elucidation and anti-microbial studies of three novel mixed ligand Schiff base complexes of copper (II), J. Serb. Chem. Soc., **72**, 983-992(2007).
36. S. Chandra, Vandana, Synthesis, spectroscopic, anticancer and antibacterial studies of Ni(II) and Cu(II) complexes with 2-carboxybenzaldehyde thiosemicarbazone, J. Spectrochimica Acta Part A, 129, 333-338(2014).
37. B.J. Hathaway, D. E. Billing, The electronic properties and stereochemistry of mono-nuclear complexes of the copper(II) ion Coordination Chemistry Reviews,5, 143-207(1970).
38. S.M.E. Khalil, ESR and spectroscopy studies of metal complexes of novel Schiff bases derived from 6- methyl-3-formyl-4-hydroxy-2-(1H) quinolone and 1,3-diamnopropane or N-(2-aminoethyl)1-,3-propanediamine. VI, J. Coord. Chem., **49,** 45-61(1999).
39. X. Wang, J. Ding, et al. Structure and magnetic properties of a neutral dimeric copper (II) complex of N-(2-hydroxybenzyl) glycinamide ligand, J. Appl. Phys., 93, 7819-7821(2003).
40. N. Aiswarya, M. Sithambaresan et al., Polymeric polymorphs and a monomer of pseudohalide incorporated Cu(II) complexes of 2,4-dichlorido-6-((2-(dimethylamino) ethyl imino) methyl) phenol]: Crystal structures and spectroscopic behavior, J. Inorganica Chimica Acta**, 443**, 251-266(2016).
41. B.G.Tweedy, Plant Extracts with Metal Ions as Potential Antimicrobial Agents, Phytopathology, **55**, 910-918(1964).
42. Z. H. Chohan, A. Munawar, C.T. Supuran, Transition Metal Ion Complexes of Schiff-bases. Synthesis, Characterization and Antibacterial Properties, J. Metal-Based Drugs, 8, 137-143(2001).
43. J. Iqbal, S.A. Tirmizi, et al. Biological properties of chloro-salicylidene aniline and its complexes with Co (II) and Cu (II), Turk. J. Biol, **30**, 1-4(2006).
44. V.B. Singh, A. Katiyar, S. Singh, Synthesis, characterization of some transition metal(II) complexes of acetone p-amino acetophenone salicyloyl hydrazone and their antimicrobial activity J. BioMetals, **21**, 491-501(2008).
45. A. Soroceanu, L. Vacareanu et al., Assessment of some application potentials for copper complexes of the ligands containing siloxane moiety: Antimicrobial, antifungal, antioxidant and redox activityJ. Inorganica Chimica Acta, **442**,119-123(2016).
46. L.H. Abdel Rahman, A.M. Abu-Dief et al., Nano Structure Iron (II) and Copper (II) Schiff Base Complexes of NNO-Tridentate Ligand as New Antibiotic Agents: Spectral, Thermal Behaviors and DNA Binding Ability Int. J. Nano. Chem.,**1**, 65-77(2015).
47. J.A. Klaus, T.M Brooks et al., Synthesis, characterization, and antimicrobial activities of palladium Schiff base complexes derived from aminosalicylic acids, J. Transition Metal Chemistry, 42, 263–271(2017).

Tables

Table 1. Analytical and physical data of Schiff base ligand (H_2L) and its metal complexes.

Compound (Molecular Formula)	Colour (%yield)	M.p. (°C)	% Found (Calcd.)				$\mu_{eff.}$ (B.M.)	Λ_m $\Omega^{-1}mol^{-1}$ cm^2
			C	H	N	M		
H_2L	yellow (90)	64	75.30 (75.32)	4.50 (4.70)	6.04 (6.06)	----	----	------
$[Cr(L)(H_2O)_2]Cl$	Green (87)	100	59.36 (59.64)	4.03 (4.11)	4.56 (4.79)	8.78 (8.91)	4.10	70
$[Mn(L)(H_2O)_2]$	Brown (85)	110	63.09 (63.16)	4.06 (4.35)	5.05 (5.08)	9.95 (9.90)	5.98	8
$[Fe(L)(H_2O)_2]Cl$	Brown (80)	118	55.11 (55.21)	3.14 (3.32)	4.16 (4.43)	9.08 (9.51)	5.08	67
$[Co(L)(H_2O)_2]$	Brown (82)	170	62.41 (62.71)	4.17 (4.32)	5.01 (5.04)	10.76 (10.61)	4.97	35
$[Ni(L)(H_2O)_2]$	Green (87)	›300	62.45 (62.73)	4.23 (4.30)	5.00 (5.04)	10.55 (10.58)	3.44	30
$[Cu(L)(H_2O)_2]H_2O$	Black Green (80)	110	60.16 (60.25)	4.36 (4.50)	4.59 (4.84)	10.98 (11.00)	1.68	38
$[Zn(L)(H_2O)_2]$	Brown (86)	184	61.63 (61.98)	4.01 (4.27)	4.53 (4.98)	11.34 (11.64)	Diam.	11
$[Cd(L)(H_2O)_2]$	Brown (83)	220	57.02 (57.19)	3.90 (3.94)	4.35 (4.60)	18.08 (18.47)	Diam.	9

Table 2. IR spectra (4000-400 cm^{-1}) of H_2L and its metal complexes.

Assignment	H_2L	[Cr(L)$(H_2O)_2$]Cl	[Mn(L)$(H_2O)_2$]	[Fe(L)$(H_2O)_2$]Cl	[Co(L)$(H_2O)_2$]	[Ni(L)$(H_2O)_2$]	[Cu(L)$(H_2O)_2$]H_2O	[Zn(L)$(H_2O)_2$]	[Cd(L)$(H_2O)_2$]
OH	3372 sh	3382 br	3472 w	3426 br	3402 br	3403 br	3403 br	3499 br	3473 s
C=O	1671 sh	1694 w	1668 w	1697 m	1689 m	1691 m	1690 s	1606 s	1671 s
C=N	1612 sh	1605 w	1591 m	1591 m	1592 s	1594 s	1594 s	1560 s	1589 s
COO_{asym}	1558 sh	1533 s	1543 s	1526 s	1537 s	1540 s	1525 m	1508 w	1555 m
COO_{sym}	1419 sh	1407 s	1458 w	1480 s	1408 s	1406 s	1455 m	1488 s	1418 s
C-O	1245 sh	1224 m	1227 m	1225 m	1226 m	1224 s	1230 m	1226 s	1246 m
H_2O stretching of coordinated water	-----	925 w 842 w	925 w 853 w	934 w 834 w	950 w 869 w	927 w 871 w	932 w 871 w	926 w 850 w	917 m 863 w
M-O	-----	564 w	556 w	564 w	562 w	564 w	568 m	583 w	566 w
M-O of H_2O coordinated	-----	520 w	532 w	543 m	522 w	516 w	545 w	539 w	529 w
M-N	-----	431 m	452 w	488 m	419 m	494 w	422 m	468 w	416 w

sh = sharp; br = broad; s = strong; m = medium; w = weak

Table 3. ^1H NMR spectral data of the Schiff base ligand (H_2L) and its Zn(II) and Cd(II) complexes.

Compound	Chemical shift, (δ) ppm	Assignment
H_2L	12.98	(s, H, OH)
	7.34 - 7.54	(m, 10H, Ar H benzoyl methane)
	7.57 - 8.18	(m, 8H, Ar H amino benzoic acid)
	4.87	(s, 2H, CH_2)
$[Cd(L)(H_2O)_2]$	Disappear	(s, H, OH)
	6.26 - 7.53	(m, 10H, Ar H benzoyl methane)
	7.56 - 8.75	(m, 8H, Ar H amino benzoic acid)
	4.87	(s, 2H, CH_2)
$[Zn(L)(H_2O)_2]$	Disappear	(s, H, OH)
	6.46 - 7.51	(m, 10H, Ar H benzoyl methane)
	7.54 - 8.17	(m, 8H, Ar H amino benzoic acid)
	4.86	(s, 2H, CH_2)

Table 4. Thermoanalytical results (TG and DTG) of H_2L ligand and its metal complexes.

Complex	TG range (°C)	DTG_{max} (°C)	n*	Mass loss mass loss Estim (Calcd) %	Total	Assignment	Residues
H_2L	152 – 367	182, 352	2	99.92 (98.71) 99.92 (98.71)		- Loss of $C_{29}H_{22}N_2O_4$.	--------
$[Cr(L)(H_2O)_2]Cl$	130 - 250 250 – 470	150, 222 415	2 1	36.54 (37.27) 43.38 (43.53) 79.93 (80.80)		-Loss of $2H_2O$, HCl, CO_2 and C_7H_3N. -Loss of $C_{18}H_{16}NO_{0.5}$.	3C+ ½ Cr_2O_3
$[Mn(L)(H_2O)]$	150 – 500	189, 453	2	80.19 (80.58) 80.19 (80.58)		- Loss of $2H_2O$, CO_2 and $C_{25}H_{20}N_2O$.	2C+MnO
$[Fe(L)(H_2O)_2]Cl$	120 - 230 230 – 586	169 401, 557	1 2	35.25 (34.98) 45.18 (45.28) 81.85 (82.07)		- Loss of $2H_2O$, HCl, CO_2 and C_6H_3N. - Loss of $C_{19}H_{16}NO_{0.5}$.	3C + ½ Fe_2O_3
$[Co(L)(H_2O)_2]$	140 - 205 205 – 432	173 392	1 1	46.86 (46.67) 31.55 (31.53) 78.41 (78.20)		- Loss of $2H_2O$, CO_2 and $C_{13}H_9N$. - Loss of CO and $C_{10}H_{13}N$.	4C +CoO
$[Ni(L)(H_2O)_2]$	140 - 265 265 – 425	172 400	1 1	49.32 (49.21) 31.40 (30.82) 80.72 (80.03)		- Loss of $2H_2O$, CO_2 and $C_{14}H_{11}N$. - Loss of $C_{11}H_9NO$.	3C + NiO
$[Cu(L)(H_2O)_2]H_2O$	60 – 115 115 – 345	89 168, 304	1 2	3.22 (3.11) 74.61 (74.79) 77.83 (77.90)		- Loss of H_2O. - Loss of $2H_2O$, CO_2 and $C_{24}H_{20}N_2O$.	4C + CuO
$[Zn(L)(H_2O)_2]$	170 - 210 210 – 650	190 352, 623	1 2	45.71 (46.13) 30.38 (30.81) 76.10 (76.94)		- Loss of $2H_2O$, CO_2 and $C_{13}H_9N$. - Loss of CO and $C_{10}H_{11}N$.	4C + ZnO
$[Cd(L)(H_2O)_2]$	150 – 240	195	1	76.52 (76.92) (76.92)	76.52	- Loss of $2H_2O$, CO_2 and $C_{27}H_{20}N_2O$.	C + CdO

Table 5. Biological activity of Schiff base ligand (H_2L) and its metal complexes with *Gram- positive* bacteria and *Gram- negative* bacteria.

Sample	Inhibition zone diameter (mm / mg sample)			
	(Gram- positive)		*(Gram- negative)*	
	Streptococcus pneumoniae	*Bacillus Subtilis*	*Pseudomonas aeruginosa*	*Escherichia coli*
Control: DMSO	0	0	0	0
H_2L	14.6±0.42	15.9±0.53	10.2±0.21	9.8±0.31
$[Cr(L)(H_2O)_2]Cl$	16.3±0.42	19.1±0.51	11.4±0.36	10.7±0.31
$[Mn(L)(H_2O)_2]$	14.6±0.58	14.3±0.58	10.2±0.31	8.8±0.24
$[Fe(L)(H_2O)_2]Cl$	17.5±0.44	19.8±0.63	15.1±0.45	18.9±0.25
$[Co(L)(H_2O)_2]$	13.8±0.40	17.2±0.43	11.6±0.36	10.9±0.21
$[Ni(L)(H_2O)_2]$	24.9±0.63	21.5±0.34	22.7±0.56	18.4±0.41
$[Cu(L)(H_2O)_2]H_2O$	22.6±0.34	33.7±0.25	13.1±0.32	15.3±0.48
$[Zn(L)(H_2O)_2]$	12.9±0.63	13.2±0.58	10.7±0.24	9.9±0.34
$[Cd(L)(H_2O)_2]$	18.2±0.68	18.9±0.64	10.8±0.41	11.1±0.43
Amikacin	9	6	7	6

Table 6. Biological activity of Schiff base ligand (H_2L) and its metal complexes with fungi.

Sample	Inhibition zone diameter (mm / mg sample)			
	(fungi)			
	Aspergillus Fumigatus	*Syncephalastrum racemosum*	*Geotricum candidum*	*Candida albicans*
Control: DMSO	0	0	0	0
H_2L	0	0	10.3±0.19	12.1±0.26
$[Cr(L)(H_2O)_2]Cl$	18.2±0.56	13.7±0.39	19.1±0.45	18.2±0.44
$[Mn(L)(H_2O)_2]$	16.3±0.35	14.8±0.46	15.3±0.52	14.3±0.58
$[Fe(L)(H_2O)_2]Cl$	15.3±0.55	13.4±0.35	11.5±0.58	13.1±0.3
$[Co(L)(H_2O)_2]$	24.1±0.51	16.9±0.52	11.5±0.43	10.8±0.46
$[Ni(L)(H_2O)_2]$	16.5±0.58	12.8±0.27	18.3±0.56	17.6±0.54
$[Cu(L)(H_2O)_2]H_2O$	11.5±0.58	17.6±0.27	26.9±0.35	16.5±0.5
$[Zn(L)(H_2O)_2]$	28.1±0.76	23.4±0.77	14.1±0.65	13.2±0.58
$[Cd(L)(H_2O)_2]$	26.3±0.73	20.9±0.61	12.6±0.54	11.2±0.44
Ketokonazole	9	9	9	9

Figures

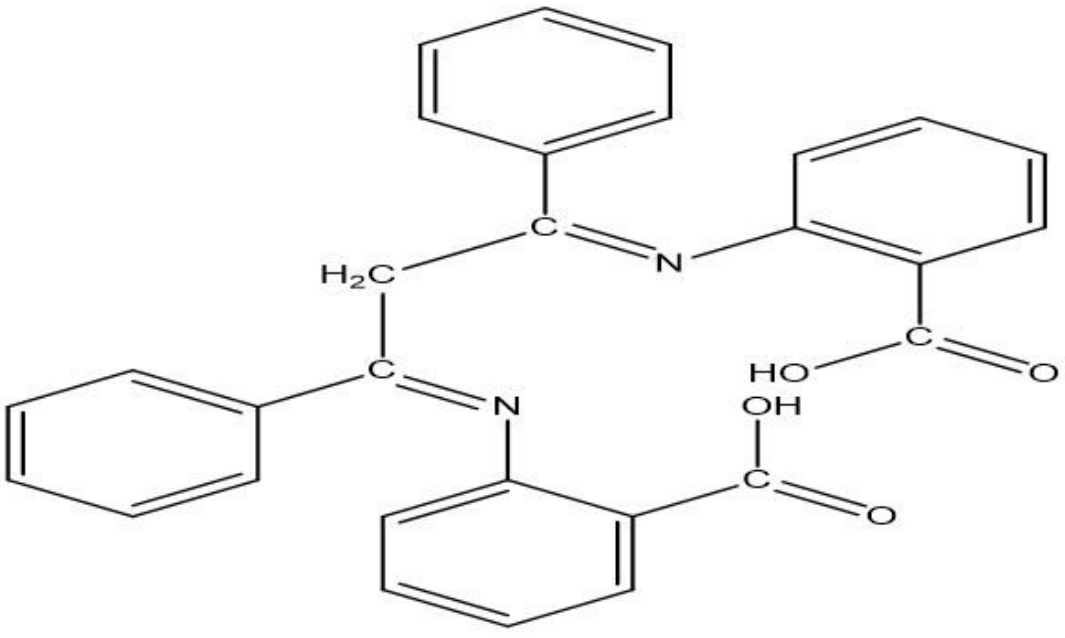

Figure 1

Structure of the Schiff base ligand2,2′-((1Z,1′Z)-(1,3-diphenylpropane-1,3-diylidene)bis(azanylylidene))dibenzoic acid (H2L).

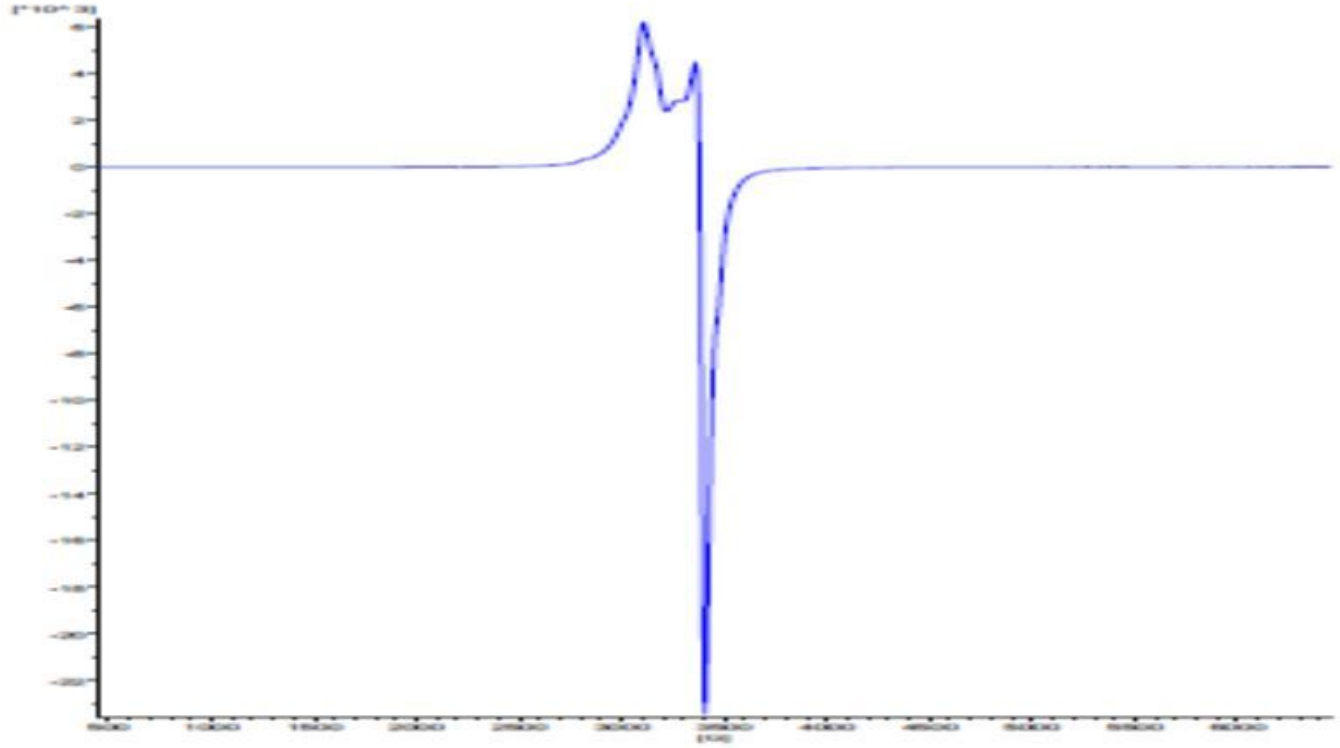

Figure 2

ESR spectrum of [Cu(L)(H2O)2]H2O complex.

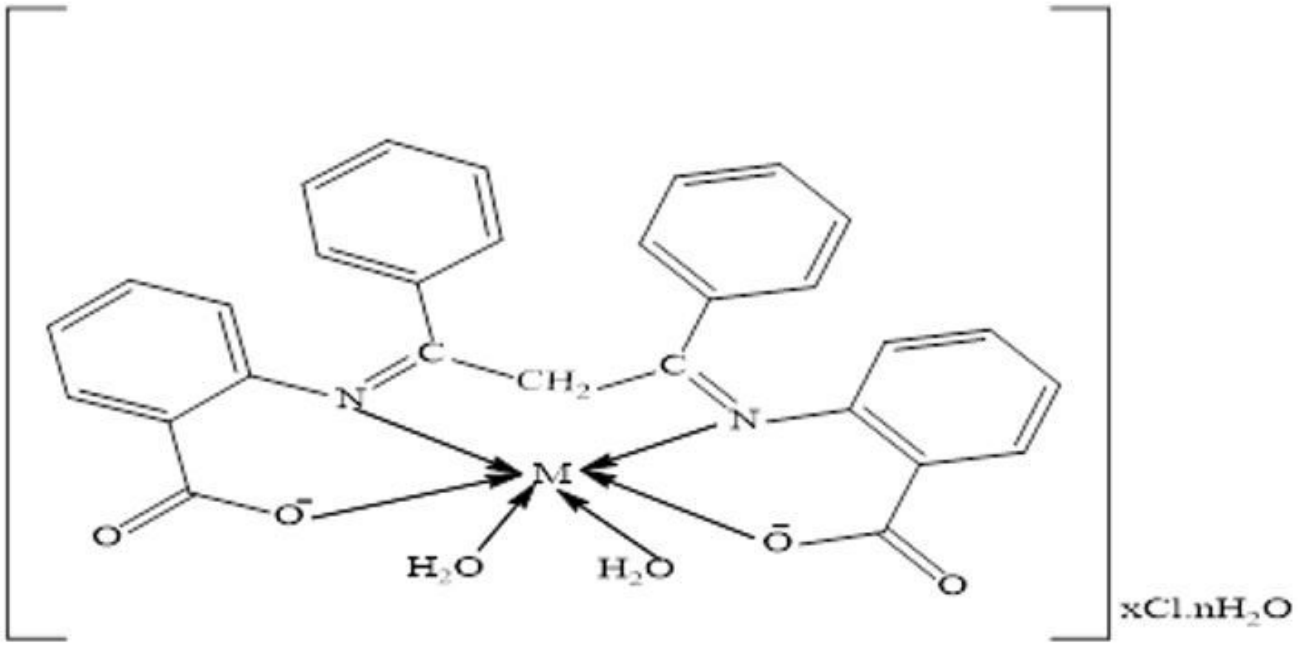

Figure 3

Structure of metal complexes of Schiff base ligand (H2L). M= Mn(II),Co(II), Ni(II), Cd(II), Zn(II) n=0, x=0; M= Cu(II) n=1, x=0; M= Cr(III), Fe(III) n=0; x=1

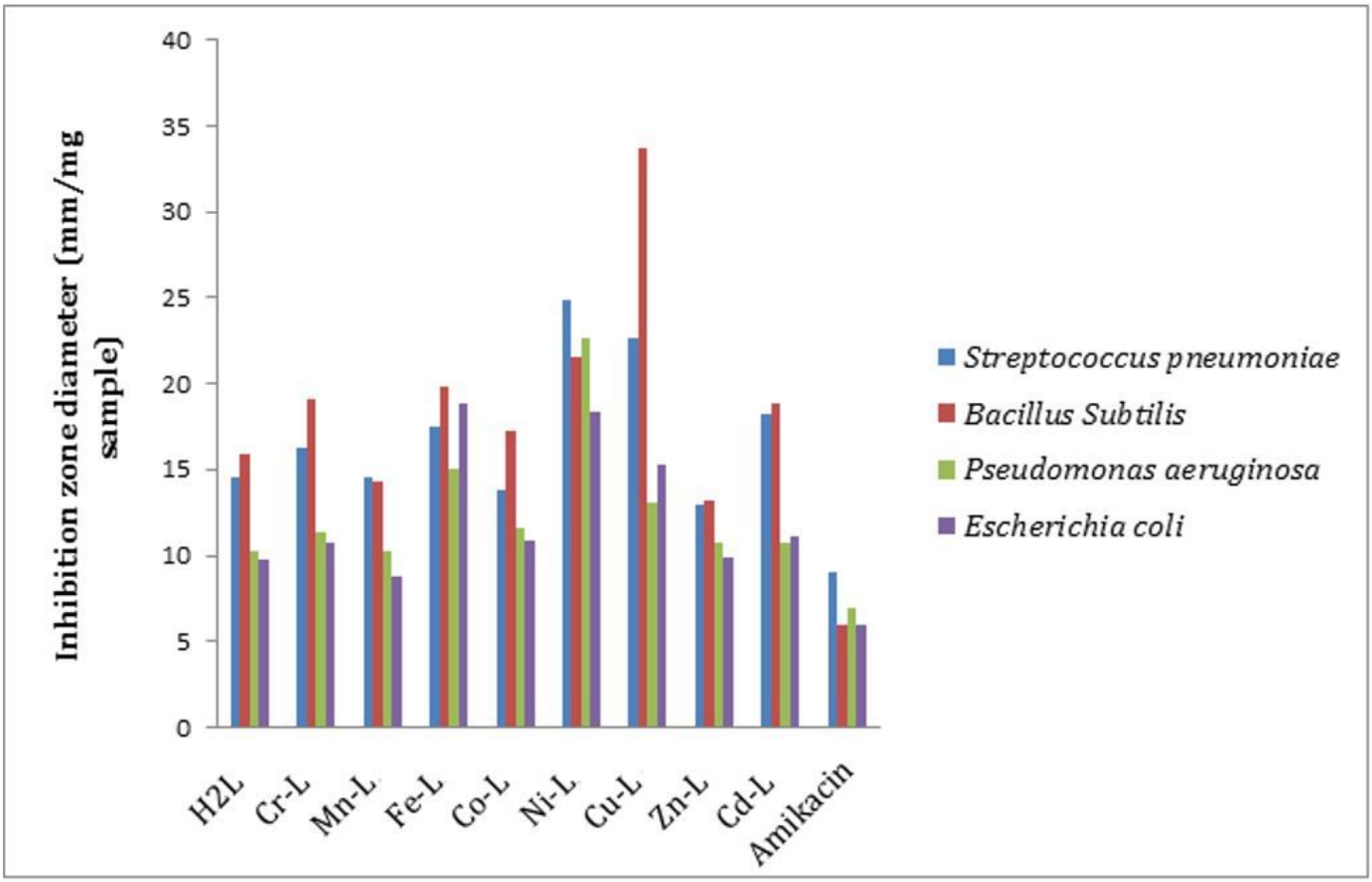

Figure 4

Biological activity of Schiff base ligand (H2L) and its metal complexes with Gram- positive and Gram-negative organisms.

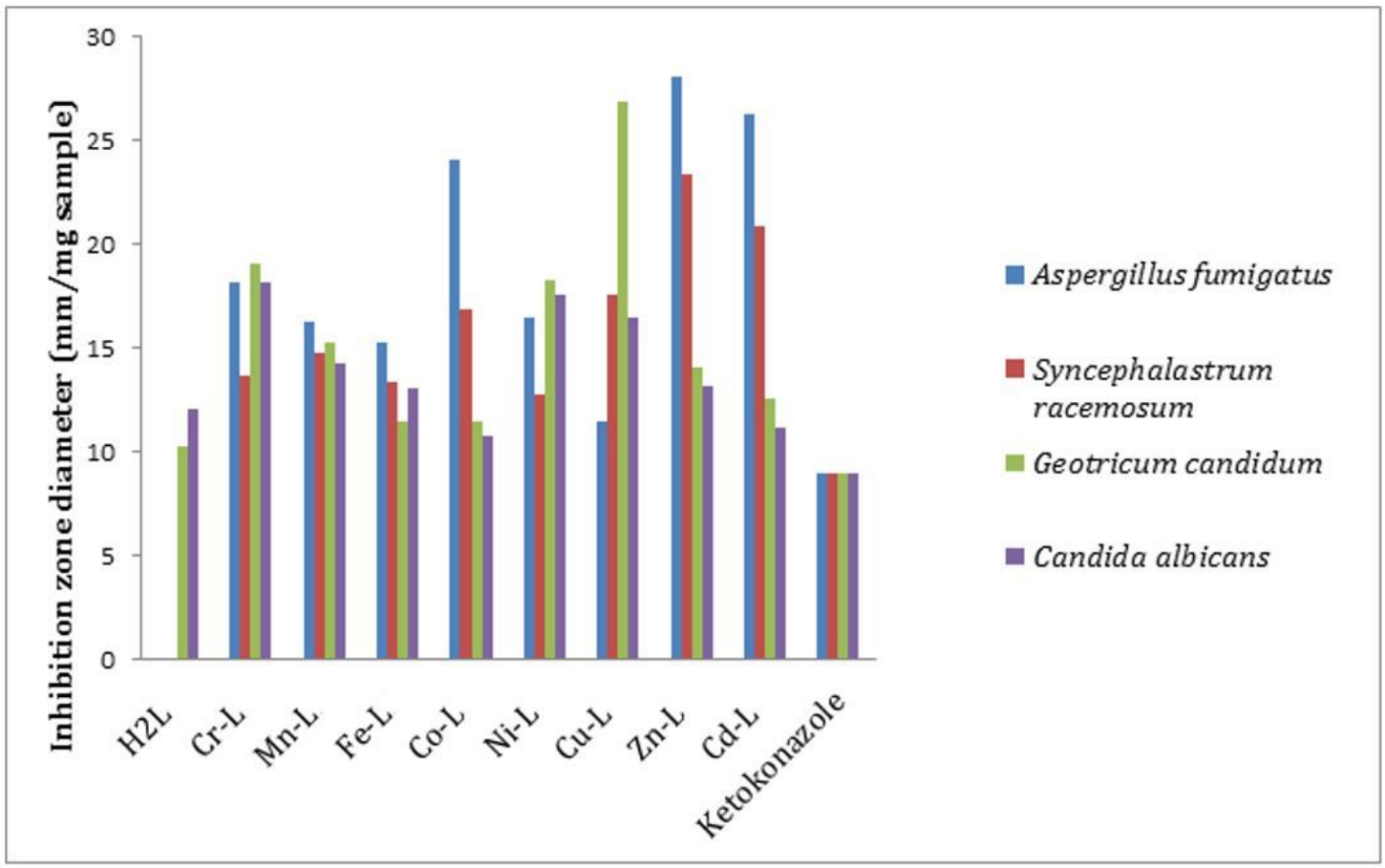

Figure 5

Biological activity of Schiff base ligand (H2L) and its metal complexes with fungi.

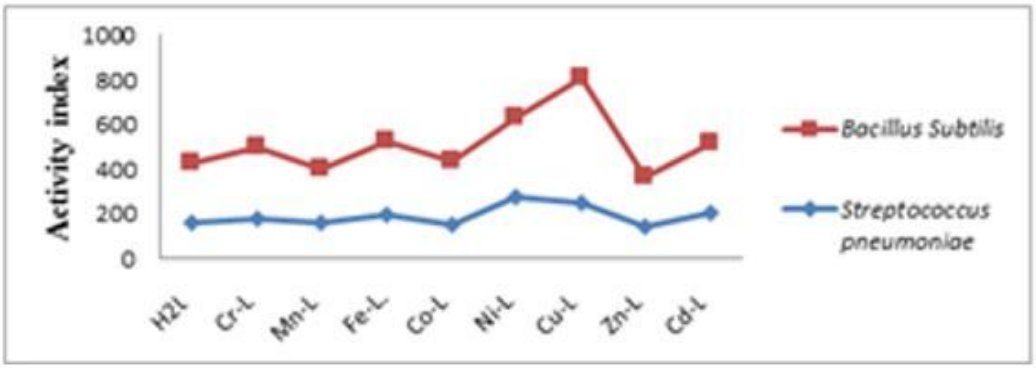

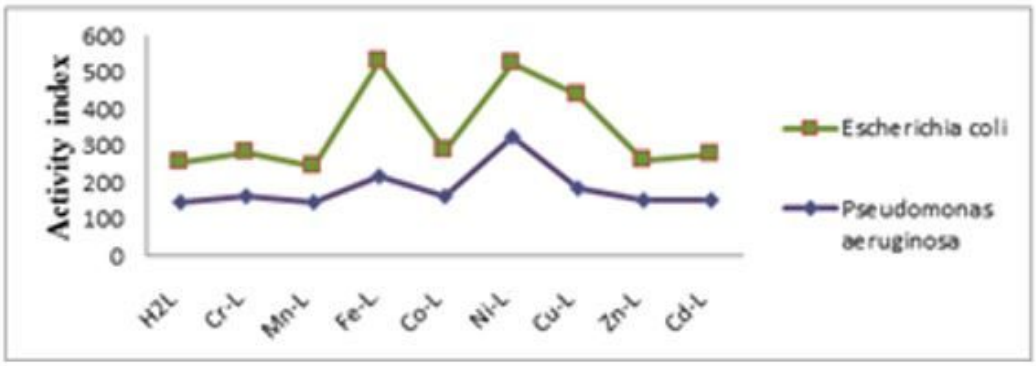

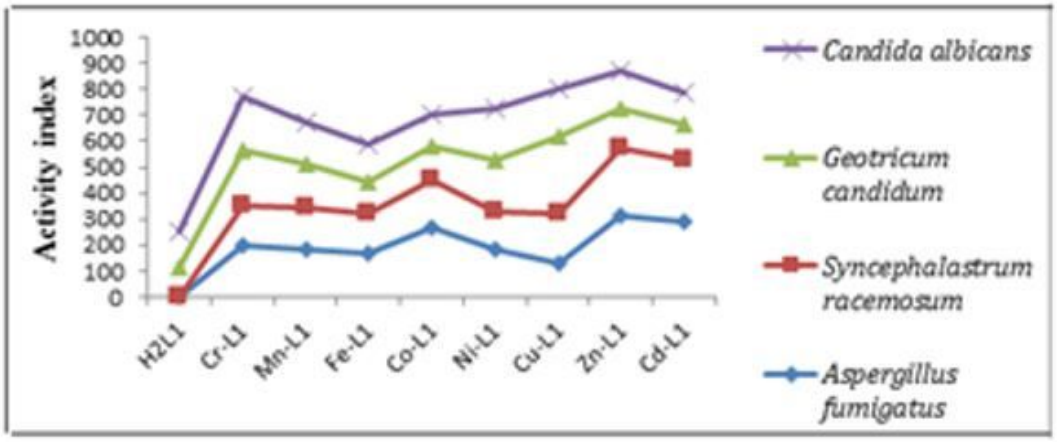

Figure 6

Activity index value of Schiff base ligand (H2L) and its metal complexes.